J. Membrane Biol. 151, 29–43 (1996)

The Journal of
Membrane
Biology

Diffusion through Narrow Pores: Movement of Ions, Water and Nonelectrolytes through Track-etched PETP Membranes

T.K. Rostovtseva,[1,*] C.L. Bashford,[2] G.M. Alder,[2] G.N. Hill,[2] C. McGiffert,[2] P.Y. Apel,[3] G. Lowe,[4] C.A. Pasternak[2]

[1]Department of Zoology, University of Maryland, College Park, Maryland, 20742
[2]Division of Biochemistry, Department of Cellular and Molecular Sciences, St. George's Hospital Medical School (University of London) London SW17 ORE (UK)
[3]Flerov Laboratory for Nuclear Reactions, JINR, Dubna, Russia
[4]Dyson Perrins Laboratory, University of Oxford, South Parks Road, Oxford OX1 3QY

Received: 14 August 1995/27 November 1995

Abstract. The rates at which ions ($^{86}Rb^+$, [^{3}H]-choline, ^{36}Cl), ^3H_2O and nonelectrolytes ([^{14}C]-urea, [^{14}C]-glycerol, and [^{14}C]-sugars) equilibrate across track-etched polyethyleneterephthalate (PETP) membranes (isotopic diffusion) have been measured by a 'static' and a 'dynamic' technique under conditions where no net flow takes place; the two techniques give essentially the same results. All tracers diffuse faster the longer the membranes are etched, consistent with an increase in pore size. Water and neutral solutes diffuse at rates that are relatively independent of ionic strength, pH or the presence of divalent cations. Diffusion of cations is decreased by high ionic strength, by reducing pH or by addition of divalent catons; diffusion of chloride is increased by these procedures. Treatment of the membrane with diazomethane to reduce the negative fixed charge decreases diffusion of cations and increases that of anions; diffusion of water and neutral solutes is unaffected by methylation except in the membranes with the narrowest pores (i.e., those etched for the shortest time), in which case diffusion is reduced. We conclude (1) that the special features of flow near a charged surface apply to ions but not to water or nonelectrolytes and (2) that calculation of absolute rates of diffusion leads to values for the radii of pores through track-etched PETP membranes that are in remarkably good agreement with measured values.

Key words: Anion diffusion — Cation diffusion — Narrow pore — Solute diffusion – Surface charge — Water diffusion

Introduction

Fluctuation of ion current through biological ion channels is generally thought to be dominated by an alteration of architecture: a change between an 'open' and a 'closed' state (Hille, 1992). Pores induced across biological membranes by certain toxins and immune molecules show fluctuations similar to those of endogenous ion channels, (e.g., Michaels, 1979; Donovan et al. 1981; Kagan, Finkelstein & Colombini, 1981; Tosteson & Tosteson, 1981; Raymond, Slatin & Finkelstein, 1985; Menestrina & Pasquali, 1985; Menestrina, 1986; Young et al., 1986; Bashford et al., 1988; Gambale & Montal, 1988) though in this instance a recent observation (Korchev et al., 1995) has thrown doubt on the concept that fluctuations between high and low conductance states necessarily reflect changes in pore size or the openings and closings of some kind of physical gate. Confirmation of the existence of such gates by structural studies has proved technically elusive — except recently in regard to the acetylcholine receptor (Unwin, 1995) —, and direct measurement of water or solute flow through channels in their 'open' and 'closed' states has — for other technical reasons — generally not been possible.

The finding that ion current through narrow pores in synthetic track-etched membranes composed of polyethyleneterephthalate (PETP) displays many of the properties of ion current through endogenous channels and

* *On leave of absence from:* Institute of Cytology, Russian Academy of Sciences, St Petersburg (Russia)

Correspondence to: C.A. Pasternak

induced pores — including fluctuations between high- and low-conducting states (Lev et al., 1993) — has opened up the possibility of using such membranes to study the effects of treatments that cause ion current to vary, on the flow of water and neutral solutes. For example, alteration of pH has a dramatic effect on ion current (Lev et al., 1993), as well as on fluctuations (Pasternak et al., 1993) just as it does on certain endogenous ion channels (Root & MacKinnon, 1994) and on 'open channel noise' in a toxin-induced channel (Kasianowicz & Bezrukov, 1995); addition of divalent cations leads to similar changes. These effects are most likely mediated by the fixed negative charges (carboxylate) at the surface of track-etched PETP membranes (Apel et al., 1985). Does altering this charge by pH or divalent cations affect the size of pores? To answer this question we have measured the diffusion of water and nonelectrolytes as well as that of cations and anions, through track-etched PETP membranes with pores of differing size. To avoid oscillations and other effects generated by chemical gradients or pressure differences (Meares & Page, 1974), we have measured the diffusion of radioactive tracers between solutions of identical composition, i.e., ''zero *cis-trans* exchange.'' Two types of experimental setup have been used: one in which the solutions on either side of the membrane remain static (except for mixing) and one in which one of the solutions flows past the other, as in flow dialysis (Colowick & Womack, 1969; Feldmann, 1978). Both give essentially the same result, which is that diffusion of water and nonelectrolyte is unaffected by pH, by the presence of divalent cations, or by the ionic strength of the medium. In contrast, the diffusion of cations and anions is altered — in opposite directions — by such treatments. We conclude that changes in ion flow resulting from alterations of pH, divalent cations or ionic strength, are due to effects on the fixed surface charge along the walls of pores and are not necessarily the result of changes in the size or accessibility of pores.

Materials and Methods

Membranes

The membranes were made of polyethyleneterephthalate (PETP; Lavsan), of thickness 10 μm, that were irradiated with Kr at 400 MeV to produce $1.03+/-0.4 \times 10^9$ tracks/cm^2 [measured by counting the number of tracks through a pack of parallel membranes, one of which was etched for a long time to make the pores visible by electron microscopy (ave radius 100–150 nm); a JSM 840 scanning electron microscope (magnification × 20,000) was used; 714 pores were counted with an accuracy of 3.7%]. The membranes were then etched in 0.2N NaOH at 80°C for varying times (5, 10, 20, 30 and 50 min). Portions of the 10-, 20- and 50-min etched membranes were further treated with diazomethane to reduce the surface charge as follows: Membranes were soaked in 0.1N HCl overnight to protonate free carboxylate groups. After 3 washes in water the membranes were dried in a dessicator (over KOH). They were then soaked in ethanol, folllowed by ether; they were then exposed to a solution of diazomethane in ether, followed by washing in ether. Control (unmethylated) filters were treated in exactly the same way, except that diazomethane was omitted during the ether treatment.

Solutions

All solutions (KCl, NaCl, choline chloride) were buffered with 0.5–5 mM Hepes to give the pH stated; pH was changed by adding KOH or HCl as appropriate. For ''static'' experiments all solutions contained 0.1 mM EDTA; the stated final concentrations of $CaCl_2$ and $ZnS0_4$ take this into account.

'Static' Experiments

Membranes were placed between two chambers (approx 5 × 4 × 20 mm) and sealed with silicon vacuum grease; the volume of solution in each chamber was 0.35 ml at the start of the experiment; the area of membrane in contact with solution was app. 1 cm^2. This is essentially the apparatus used for measuring current across the membranes at various applied voltages in the presence of Pt or Ag/AgCl electrodes (Lev et al., 1993) and was used for the measurement of reversal potential (*see below*).

Identical solutions of varying ionic strength and pH were placed in each chamber; to one chamber (''hot'' side) appropriate tracer was added. All tracers were obtained from Amersham International. The solution in each chamber was mixed and a sample (generally 5 μl) removed from each side at intervals and its radioactivity assessed. From measurements over a time span during which radioactivity appearing in the 'cold' chamber was linear with time, the rate of diffusion, K_d was calculated; K_d = 2 × cpm ''cold side''/cpm ''cold & hot''/min/cm^2. All experiments were carried out at room temperature (22–25°C).

'Dynamic' Experiments

Membranes were placed in a chamber (Feldmann, 1978) designed to measure the rate of dialysis of radiochemical tracers; this procedure (''flow dialysis'') was originally devised to measure the binding of ligands to macromolecules (Colowick & Womack, 1969). The upper chamber, which was stirred continuously with a magnetic 'flea,' contained 0.5 ml of the solution containing the appropriate tracer; an identical solution without tracer was pumped through the spirally wound lower chamber at a constant rate using a microperpex 2 peristaltic pump (LKB) and was collected as 0.5 ml fractions. The area of membrane in contact with solution was 0.5 cm^2. Radioactivity was assessed in each fraction; from time to time 5 μl samples were taken from the upper chamber to measure its radiochemical content. The rate of diffusion was calculated as the quotient of counts in each fraction/counts in the upper chamber, divided by the time taken to collect each fraction and averaged over the entire run; this value, which is essentially a first order rate constant, was used for the rate of diffusion, K_d. Experiments were carried out at room temperature (22–25°C).

Calculation of Selectivity

Selectivity of ion diffusion (sel_d) was calculated from the relative rates of diffusion such that:

$$sel_d = K_{d(\text{cation})}/(K_{d(\text{cation})} + K_{d(\text{anion})})$$

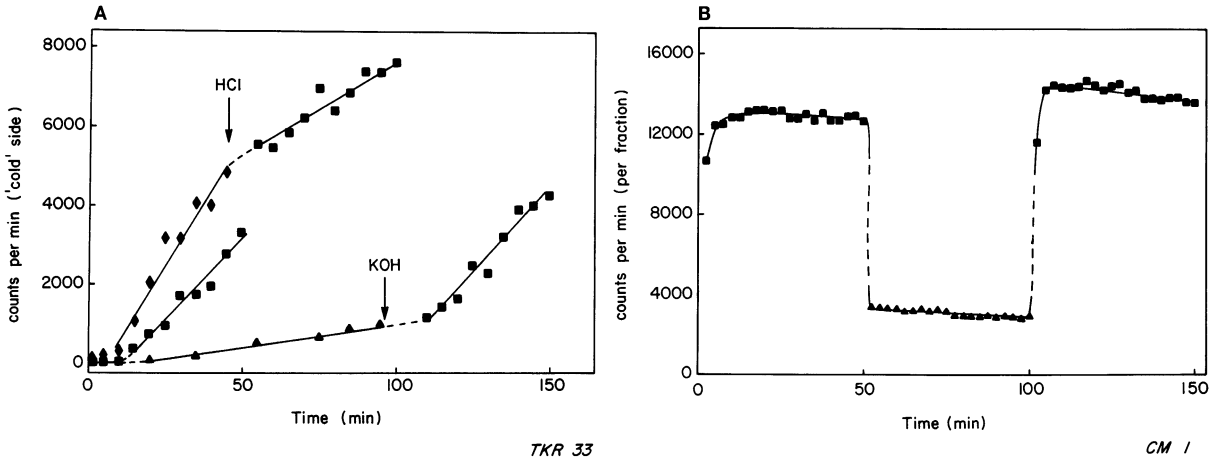

Fig. 1. Diffusion of ^{86}Rb across track-etched PETP membranes. 'Static' experiments (Panel *A*): the membrane, etched for 20 min, was placed between solutions containing 0.01 M KCl, 0.0005 M Hepes, 0.0001 M EDTA, pH adjusted to 3 (▲), 7.5 (■), or 11 (♦); the arrows indicate the addition of HCl or KOH to both chambers to bring the pH to its new value. The 'hot' side contained 4×10^6 dpm ^{86}Rb/ml at the commencement of each experiment. Three separate experiments are presented. 'Dynamic' experiments (Panel *B*): the membrane had been etched for 20 min; the solutions in both chambers contained 0.01 M KCl and phosphate/citrate buffer diluted 1:100 to give final pH values of 7.4 (■) or 3.2 (▲); the upper chamber contained 4×10^6 dpm ^{86}Rb/ml at the start of each phase; after 20 fractions had been collected solutions in upper and lower chambers were replaced by fresh solutions of differing pH.

Selectivity of ion current (t_+) was calculated from measurement of the reversal potential (voltage, Ψ, required to prevent ion current from flowing when the two chambers in 'static' experiments contain KCl solutions of differing ionic strength) by the formula:

$$t_+ = \tfrac{1}{2}\,[1 + \Psi/\{(RT/F)\ \ln\ ([K^+]\ trans/[K^+]\ cis)\}]$$

where R, T and F have their usual meanings (Appendix 1). t_+ was measured either across ~1 cm^2 pieces (containing 10^9 pores) of membrane essentially as described by Lev et al. (1993) or across individual ~1 μm^2 patches (containing 1–10 pores) in such membranes by applying a patch pipette to the surface of a piece of membrane floating on a solution in which a second electrode was immersed (Pasternak et al. 1995*a*); the patch pipette contained the less concentrated of the two solutions. Values without parentheses refer to the former method; values with parentheses (number of measurements) refer to individual patches.

For ions such as Rb^+ or K^+ and Cl^- that have approximately the same diffusivity in aqueous solution, sel_d and t_+ are equal, and a value of $sel_d = 0.5$ indicates zero selectivity. For ions of differing diffusivity such as choline and Cl^- the value of sel_d at which their rates of diffusion through a pore are effectively the same (zero selectivity) will not be 0.5; in the case of choline and Cl^- it is 0.33 [taking a value of 1 for the diffusion coefficient of choline (mol. wt. 104); we base this value on the fact that the diffusion coefficients of the chemically similar compounds TMA (mol. wt. 74) and TEA (mol. wt. 130) are 1.19 and 0.87 resp. (p. 268 of Hille, 1992)].

Estimation of Pore Size

Pore size was estimated by the solute penetration technique of Krasilnikov et al. (1988, 1992). This depends on the assumption that nonelectrolyte solutes that are able to penetrate a pore lower the conductance at a particular voltage whereas nonelectrolytes that are unable to penetrate a pore do not affect the conductance. The following nonelectrolytes (at 20% w/w) were added to the chambers used for 'static' experiments (each chamber also contained 0.1 M KCl, 5 mM phosphate/citrate buffer and 1 mM EDTA pH 7.0): glycerol (mol. wt. 92) and polyethyleneglycols of mean mol. wt. 300, 600, 1,000, 2,000, 4,000, 10,000, 20,000 and 35,000; conductance at an applied AC voltage of 4.5V (1 kHz) was then measured. The relative penetration, A was calculated from the formula:

$$A = [G_{mem}/G^{sol}_{mem} - 1]/[G/G^{sol} - 1]$$

where G_{mem} and G^{sol}_{mem} are the conductances through the membrane in the absence and presence of solute respectively, and G and G^{sol} are the conductances through the solution without a membrane in the absence and presence of solute respectively.

We assume that hydrated PEGs are spherical (Powell, 1980) and compute pore radii accordingly (Kuga, 1981) though we appreciate that this is an approximation (Deen, 1987).

Results

Comparison between ''Static'' and ''Dynamic'' Experiments

Typical time courses, from which initial rates of diffusion, K_d, were computed, are shown in Fig. 1. In ''static'' experiments the values of radioactivity are cumulative (and will tail off as equilibrium is reached when 50% of tracer has reached the ''cold'' side); in ''dynamic'' experiments, each sample in effect indicates the initial (or fractional extraction) rate.

It is a property of lightly etched PETP membranes that when they are first used from the dry state, the rates of ion, water and solute diffusion are higher than after they have been kept under water or buffer for some time;

Table 1. Comparison between ''static'' and ''dynamic'' techniques for measurement of rates of diffusion

Tracer	''Static'' technique		''Dynamic'' technique	
	K_d ($min^{-1} \cdot cm^{-2}$)	Relative rate	K_d ($min^{-1} \cdot cm^{-2}$)	Relative rate
$^{86}Rb^+$	$9.5 \pm 1.5 \times 10^{-3}$ (9)	100	8.35×10^{-3}	100
$^{36}Cl^-$	$5.0 \pm 0.29 \times 10^{-4}$ (3)	5.3	2.6×10^{-4}	3.1
^3H_2O	$2.1 \pm 0.33 \times 10^{-3}$ (18)	22	2.15×10^{-3}	26
[^{14}C]MeGlc	$3.6 \pm 1.0 \times 10^{-4}$ (3)	3.8	2.3×10^{-4}	2.7
Sel_d (Rb^+ *vs.* Cl^-)	0.95		0.97	

All experiments were performed on pieces of 20-min-etched PETP membrane in 0.01 M KCl, pH 7.5. The values for ''static'' experiments are given ± SD (number of experiments). The values for ''dynamic'' experiments are for a single run in each case.

swelling of the polymer, thus narrowing the pores, is likely to account for this. Also, different areas of the same membrane may show different rates: pieces near the edge of a sample may not be irradiated, i.e., ''tracked,'' as well as those in the center, and therefore the density of tracks — and hence the density of pores after etching — may be less. Despite variation in absolute rates from piece to piece, or from day to day, the relative rates for different ions and solutes, and hence properties such as selectivity, remain remarkably constant. For example, a particular piece of 20-min etched membrane had the properties indicated in the left-hand column of Table 1 when examined by the ''static'' technique. In another piece, measured in an identical manner on a subsequent occasion, the rates of Rb^+, Cl^- and MeGlc diffusion had decreased 100 times and water diffusion had decreased 10 times, whereas the ratio of Rb^+ to Cl^- was unchanged (sel_d 0.95).

The rates of diffusion presented in this paper are generally for pieces of membrane taken from adjacent areas that had been treated as follows: they were rinsed in water, followed by ethanol, followed by blotting and drying in air. They were kept in the dry state prior to use; once they were immersed in buffer and placed in the apparatus, measurements were made immediately thereafter.

Given the provisos mentioned above, the agreement between ''static'' and ''dynamic'' experiments was good (Table 1). Because the latter method is semi-automated and somewhat faster, as well as the fact that there is no deviation from linearity as equilibrium between ''hot'' and ''cold'' sides is approached, it is the preferred method and most results reported in this paper are taken from ''dynamic'' experiments.

Diffusion of Ions

$^{86}Rb^+$ was used throughout as tracer for K^+, once it was confirmed that the diffusion of $^{86}Rb^+$ is the same in solutions of NaCl, KCl or RbCl. Experiments with [^{3}H] choline showed a rate of diffusion some 30% that of $^{86}Rb^+$, which is compatible with its lower mobility, i.e., diffusion coefficient D, in free solutions [estimated to be approx 50% that of Rb^+ ($D = 2.07$), namely $D = 1$, for the reasons mentioned in Materials and Methods]. Diffusion of choline was generally somewhat slower in KCl (i.e., tracer choline) than in choline chloride, perhaps due to inhibition of tracer choline diffusion by K^+. The advantage of using [^{3}H] choline over $^{86}Rb^+$ as a typical cation is that ^{3}H can be measured simultaneously with

Table 2. Effect of ionic strength, pH and divalent cations on diffusion of ions

Tracer	Condition	Ionic strength		
		0.01	0.1	0.16
		(Relative K_d)		
$^{86}Rb^+$	pH 7.5	100*	31	40 (4)
	+1 mM Ca^{2+}	51		
	+10 mM Ca^{2+}	44		
	+1 mM Zn^{2+}	28 (2)		28
	pH 3	14 (3)		
	pH 11	171 (3)		
[^{3}H]Choline	pH 7.5	100*	48	49 (13)
	+1 mM Zn^{2+}	44 (2)		31 (9)
	pH 4.5			41 (2)
	pH 3	24	27	
$^{36}Cl^-$	pH 7.5	100*	197	326 (10)
	+1 mM Zn^{2+}	160 (2)		172 (5)
	pH 4.5			479
	pH 3	305 (6)	340 (2)	
	pH 11	102		

All experiments were performed on pieces of 20-min-etched PETP membrane in 0.01 M salt (KCl or choline), 0.1 M salt (KCl or choline Cl) or 0.16 M salt (NaCl, KCl or choline Cl) at the pH indicated. $CaCl_2$ or $ZnSO_4$ was added to the final concentration shown. The rate of diffusion, K_d, was determined by either the ''static'' or the ''dynamic'' techniques using a single piece for all ''dynamic'' measurements. Where more than one experiment was performed, the number is given in parentheses.

* K_d values (±SD) were as follows: $^{86}Rb^+$: $9.3 \pm 1.4 \times 10^{-3}$ (11) $min^{-1} \cdot cm^{-2}$; [^{3}H]choline: $1.71 \pm 0.14 \times 10^{-3}$ (3) $min^{-1} \cdot cm^{-2}$; $^{36}Cl^-$: $4.0 \pm 0.2 \times 10^{-4}$ (5) $min^{-1} \cdot cm^{-2}$.

Table 3. Effect of ionic strength, pH and divalent cations on ionic selectivity

Panel A Ions	Condition	Ionic strength		
		0.01	0.1	0.16
		(sel_d)		
$^{86}Rb^+$ *vs.* $^{36}Cl^-$	pH 7.5	0.96	0.78	0.74
	+1 mM Zn^{2+}	0.80		0.79
	pH 3	0.52		
	pH 11	0.97		
[^{3}H]choline *vs.* $^{36}Cl^-$	pH 7.5	0.87 (3)	0.61	0.50 (6)
	+ 1 mM Zn^{2+}	0.64 (2)		0.40 (5)
	pH 3	0.22	0.34	0.40 (2)

Panel B Ions	Condition	Ionic gradient			
		0.001/0.01 *M*	0.01/0.1 M	0.1/0.3 M	0.3/3 M
		(t_+)			
K^+ *vs.* Cl^-	pH 7.5	0.92	0.88	0.77 ± 0.03 (23)	0.73
Choline *vs.* Cl^-	pH 7.8			0.88 ± 0.07 (15)	
	pH 5.5			0.67 ± 0.01 (9)	

All experiments were performed on pieces of 20-min-etched PETP membrane.
Panel A: For $^{86}Rb^+$ *vs.* $^{36}Cl^-$, the values of sel_d were calculated from the values of K_d given in Table 2. For [^{3}H]choline *vs.* $^{36}Cl^-$, the values of sel_d were calculated from individual ''double label'' experiments (number in parentheses) carried out by the ''dynamic'' technique on the same piece of membrane in which K_d for [^{3}H]choline and $^{36}Cl^-$ was measured simultaneously.
Panel B: Selectivity of ion current, t_+, was measured and calculated as described in Materials and Methods. Single values refer to measurement of reversal potential across a 1 cm^2 piece (10^9 pores); values for several experiments (in parentheses) refer to measurement of reversal potential across an app. 1 μm^2 patch (1–10 pores).

$^{36}Cl^-$, allowing direct comparison of cation and anion diffusion to be made in a single experiment. It is clear from Table 1 that the rate of diffusion of Rb^+ in 0.01 M KCl is some 20–30 times greater than that of Cl^-. Increasing the ionic strength decreases diffusion of Rb^+ and increases that of Cl^-; the effect on diffusion of choline is similar to that for Rb^+ (Table 2). This decrease in the diffusion of cations with increasing ionic strength is compatible with the relatively small increase of ion current (that is carried largely by cations in narrow track-etched PETP membranes) in response to increasing ionic strength (at pH >7.5) (Fig. 2 of Lev et al., 1993), whereas in free solution the exponential of ion current is proportional to the exponential of ionic strength (with a slope of 1).

Again, consistent with the effects of low pH and divalent cations on ion current (Lev et al. 1993), the rates of diffusion of Rb^+ and choline are each decreased by divalent cations — with Zn^{2+} more effective than Ca^{2+} — as well as by lowering pH (Table 2). These effects are more marked at low ionic strength (0.01 M) than at higher ionic strength (0.16 M).

In contrast to these effects on the diffusion of cations, those on the diffusion of anions like Cl^- — which it is not possible to predict from ion current data — are the opposite: increasing ionic strength increases the rate of diffusion, as do low pH and divalent cations (Table 2). The changes in relative diffusion of cations and anions are reflected in an altered selectivity (Table 3). The selectivity — between Rb^+ and Cl^- or between choline and Cl^-— is greatest at low ionic strength and high pH; increasing ionic strength, addition of divalent cations, or reducing pH, all decrease selectivity. Note that selectivity values of <0.5 for choline chloride in the presence of 1 mM Zn^{2+} or at low pH do not imply that the surface becomes positively charged under these conditons. Because the mobility of choline is less than that of Cl^-, a sel_d of 0.33 corresponds to that expected in free solution; the reason for the value of 0.22 at pH 3 is not at present clear. The effect of altering ionic strength is clearly indicated in Fig. 2, where its effect on diffusion of choline and Cl^- is compared with that on diffusion of water and glycerol (*see below*). The values of sel_d, based on rates of diffusion, are in reasonable agreement with values of t_+, based on reversal potential between solutions of differing ionic strength and pH (Table 3). The effect of pH on sel_d and t_+ is more clearly shown (for two membranes etched for shorter times) in Fig. 3; addition of divalent cations

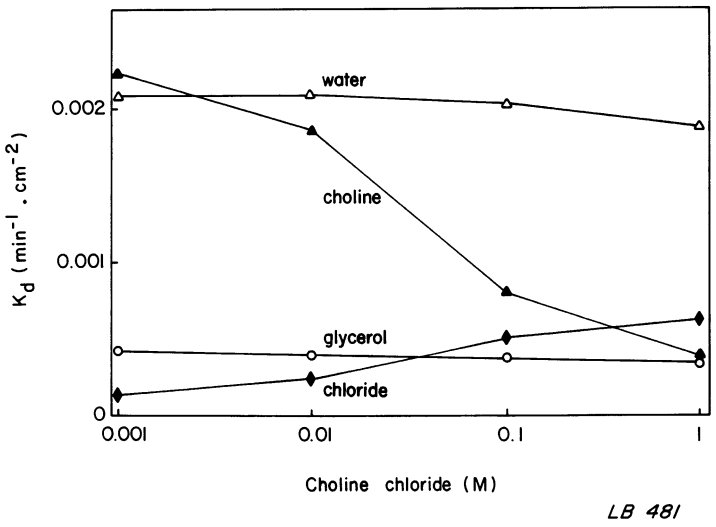

Fig. 2. Effect of ionic strength on diffusion of solutes across a track-etched PETP membrane. Diffusion of ^3H_2O (△), [^{3}H]-choline (▲), [^{14}C]-glycerol (O) and $^{36}Cl^-$ (♦) across a 20-min-etched membrane was determined using the dynamic technique with media containing 0.01, 0.1 or 1M choline chloride buffered with 0.005 M Hepes pH adjusted to 7.5 with NaOH or 0.001 M choline chloride buffered with 0.001 M Hepes pH adjusted to 7.5 with NaOH. The results of two experiments are presented in which the upper chamber contained either ^3H_2O with [^{14}C]-glycerol or [^{3}H]-choline with $^{36}Cl^-$.

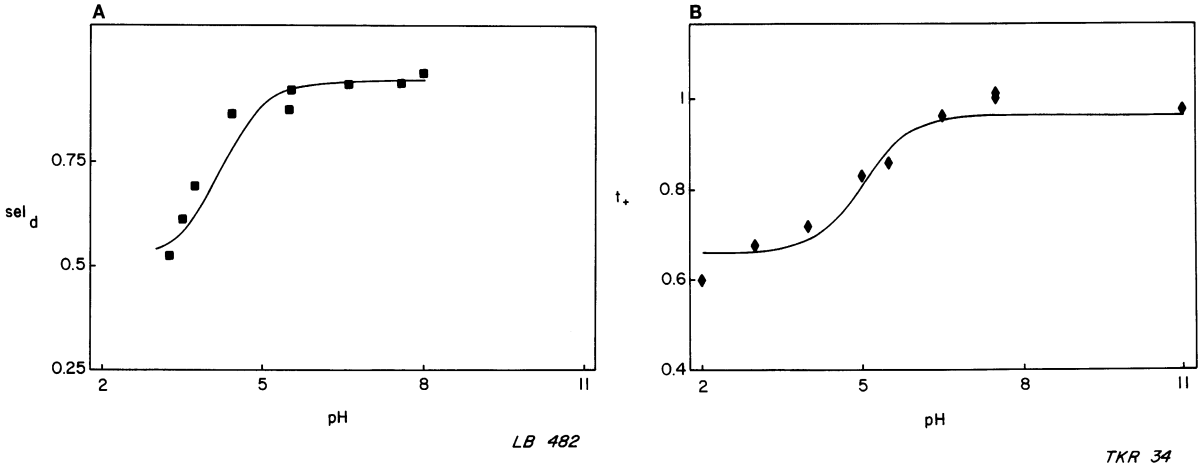

Fig. 3. Effect of pH on sel_d and t_+ in track-etched PETP membranes. sel_d (panel *A*, (■)), for [^{3}H]-choline and $^{36}Cl^-$, of a membrane etched for 10 min was determined with the 'dynamic' technique using media which contained 0.01 M choline chloride buffered with phosphate/citrate diluted 1:100 to give the pH value indicated. t_+ (panel *B*, (♦)), of a membrane etched for 5 min, was determined from the reversal potential found for a fivefold (0.1/0.5 M) gradient of KCl; each solution also contained 0.005 M Hepes and 0.001 M EDTA and HCl or KOH to give the pH value indicated. The solid curves represent the best-fit Henderson-Hasselbalch functions to the data points with the following parameters: sel_d (panel *A*) pK = 4.19 ± 0.14 with end points of 0.93 ± 0.004 (alkali) and 0.51 ± 0.03 (acid); t_+ (panel *B*) pK = 5.02 ± 0.03 with end points of 0.96 ± 0.01 (alkali) and 0.66 ± 0.01 (acid).

causes a reduction in sel_d and t_+ similar to that caused by lowering pH (*not shown*). The pattern of response to altered pH is similar for sel_d and t_+ and each fits a Henderson-Hasselbach equation for a single type of ionizable group remarkably well, with pK values of approx. 4 for the 10-min etched membrane and 5 for the 5-min etched membrane. Ion current (and diffusion of tracer cations) are also progressively more sensitive to pH, the shorter the time of etching: the pH values at which ion current is half that at pH 11 are approx. 6, 6.5, 8 and 9 for membranes etched for 50, 20, 10 and 5 min respectively. In contrast to the effect of etching time on the pH dependence of selectivity or ion current, there is little effect of ionic strength: curves for other ionic strengths are virtually superimposable on those shown in Fig. 3, and the same is true for ion current (Fig. 4 of Lev et al., 1993).

Table 4. Effect of ionic strength, pH and divalent cations on diffusion of water and nonelectrolytes

Tracer	Condition	Ionic strength		
		0.01	0.1	0.16
		(relative K_d)		
^3H_2O	pH 7.5	100*	95 (2)	120 (7)
	+10 mM Ca^{2+}	72 (3)		
	+1 mM Zn^{2+}	72 (10)		110 (2)
	pH 3	76 (7)	93	
	pH 11	115 (5)		
[^{14}C]urea	pH 7.5	100*		
	+1 mM Zn^{2+}	91 (2)		
	pH 3	94 (2)		
	pH 11	74		
[^{14}C]glyerol	pH 7.5	100*	68	60
	+1 mM Zn^{2+}	63 (2)		
	pH 3	148		
	pH 11	69		
[^{14}C]MeGlc	pH 7.5	100*		95 (3)
	+10 mM Ca^{2+}	81 (2)		
	+1 mM Zn^{2+}	77		71
	pH 3	86 (2)		
	pH 11	100		
[^{14}C]sucrose	pH 7.5	100*		72
	+10 mM Ca^{2+}	88		
	pH 3	100		
	pH 11	100		

All experiments were performed on pieces of 20-min-etched PETP membrane as described in the legend to Table 2, using the same piece for all ''dynamic'' measurements.

* K_d values were as follows: ^3H_2O: $2.1 \pm 0.33 \times 10^{-3}$ (19) $min^{-1} \cdot cm^{-2}$; [^{14}C]urea: 1.0×10^{-3} (4) $min^{-1} \cdot cm^{-2}$; [^{14}C]glycerol: 5.7×10^{-4} (3) $min^{-1} \cdot cm^{-2}$; [^{14}C]MeGlc: 3.0×10^{-4} (9) $min^{-1} \cdot cm^{-2}$; [^{14}C]sucrose: 2.1×10^{-4} (3) $min^{-1} \cdot cm^{-2}$.

A change in selectivity based on ion current as a function of pH is typical of toxin-induced pores also (e.g., Varanda & Finkelstein, 1980).

It is possible to interpret these results in terms of the surface charge due to the carboxylate groups generated by etching with alkali: cations are attracted over anions, and this results in a faster rate of diffusion of Rb^+ or choline compared with Cl^- because the concentration of mobile cations in the pores exceeds that of the mobile anions.

Diffusion of Water and Nonelectrolytes

In contrast to the diffusion of ions, the diffusion of water is relatively unaffected by pH, by divalent cations, or by ionic strength (as previously noted by Bean, 1972); there is at best a 30% change by pH, divalent cations or ionic strength (Table 4, Fig. 2) compared with 5–10-fold changes in the case of ions.

The diffusion of nonelectrolytes is likewise unaffected by pH, by divalent cations, or by ionic strength (Table 4). The rate of diffusion was unaffected by addition of unlabeled solute (10 mM) to the labeled solution (10 μM). Only in one series of experiments, with one particular piece of membrane used in the ''static'' mode — was diffusion of glycerol, MeGlc or sucrose inhibited more than app. 30% by 1 mM Zn^{2+}. On that occasion, K_d values as low <10% of those in the absence of Zn^{2+} were recorded; addition of 1 mM EDTA restored the rate to its value in the absence of Zn^{2+} in each case. Diffusion of water (in double-labeled experiments) was normal, and diffusion of MeGlc or surcrose was unaffected by 10 mM Ca^{2+} or by pH. The reason for this series of observations is not clear; similar effects of Zn^{2+} were not seen on any subsequent occasion and may be related to the possibility that the pH inside the pores had risen to the point where some Zn^{2+} had precipitated, with possible narrowing of pores.

The transport of water and nonelectrolyte such as MeGlc was measured under conditions where a voltage gradient is applied across the membrane at the same time as tracer measurements are made (by the ''static'' technique). Under these conditions, flow of ions is affected markedly. For example, application of −70 mV (the polarity being such as to attract cations from the ''hot'' chamber to the ''cold'' chamber) increases the rate of isotopic equilibration for $^{86}Rb^+$ in 0.01 M KCl, pH 7.5 some 4-fold. Application of −700 mV increase it 50-fold; under such conditions there is net movement of K^+ (measured by atomic absorption) of ~50 μM/min. The rate of isotopic equilibration for ^3H_2O or [^{14}C] MeGlc in 0.01 M KCl, pH 7.5 is unaffected by application of −700 mV. This result suggests that electro-osmosis is negligible in this system; the conclusion that voltage is without effect on the diffusion of water or nonelectrolyte is compatible with the lack of effect of ionic strength, pH or divalent cations.

Effect of Etching Time

The data presented so far refer to membranes that had been etched for 20 min. The effect of etching for only 10 min, or for etching for 50 min, on rates of diffusion in 0.16 M salt is shown in Table 5. All rates of diffusion increase, compatible with an increase in pore size. This is also suggested by experiments using the PEG exclusion technique illustrated in Fig. 4; it is difficult to calculate an exact pore size since the technique does not yield a sharp ''cutoff'' size for PETP membranes, in the way that, for example, it does for toxin-induced pores (Krasilnikov et al., 1992; Korchev et al., 1995). This is probably related primarily to the fact that the pores through PETP membranes are some 1,000 longer than those through biological membranes, and their shape is not that of a uniform cylinder, but rather that of an elongated ''egg-

Table 5. Effect of etching time on diffusions of ions and water

Tracer	Time of etching		
	10 min	20 min	50 min
$^{86}Rb^+$	1.6×10^{-4} (8)	$3.2 \pm 1.3 \times 10^{-3}$ (5)	2.1×10^{-2}
[^{3}H]choline	1.6×10^{-5} (3)	$8.2 \pm 2.1 \times 10^{-4}$ (13)	6.9×10^{-3} (2)
$^{36}Cl^-$	1.6×10^{-5} (6)	$1.3 \pm 0.8 \times 10^{-3}$ (9)	1.1×10^{-2} (5)
^3H_2O	2.9×10^{-4} (5)	$2.6 \pm 1.1 \times 10^{-3}$ (7)	1.9×10^{-2} (4)
	(Relative rate)		
$^{86}Rb^+$	0.8	15	100
[^{3}H]choline	0.2	14	100
$^{36}Cl^-$	0.15	12	100
^3H_2O	1.5	14	100

Three PETP membranes were etched for the times indicated and experiments performed on a single piece from each membrane. All experiments (number in parentheses if more than one; ±SD where appropriate) were carried out in 0.16 M salt (KCl, NaCl or choline chloride) at pH 7.5 by the ''dynamic'' technique.

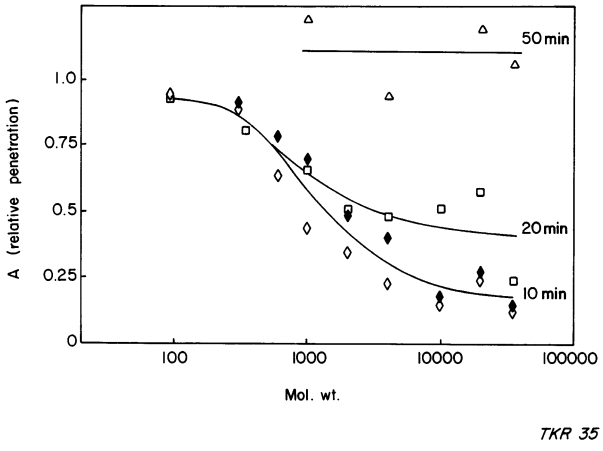

Fig. 4. Estimation of pore size in track-etched PETP membranes by PEG penetration. Membranes etched for 10 (◇, ◆), 20 (□) or 50 (△) min were bathed with solutions containing 0.1 M KCl, 0.005 M phosphate/citrate buffer, 0.001 M EDTA pH 7.0 in the absence or presence of 15–25% w/v nonelectrolytes (glycerol, sucrose or polyethyleneglycols of mean molecular weight 300, 600, 1,000, 2,000, 4,000, 10,000, 20,000 and 35,000); a methylated membrane (◆) was also assessed. Relative penetration (*A*) was estimated as described in Materials and Methods.

timer'' (*see below*); it is not related to heterogeneity of size among different pores, since a similar diffuseness of ''cutoff'' size is seen when single pores through PETP membranes are analyzed (Lev et al., 1993).

Table 5 (and Table 7, below) indicate that in the 50-min etched membrane, the different diffusion rates for ions (in 0.16 M salt) and solutes depend predominantly on their diffusivity in free solution and are relatively unconstrained by the dimensions or surface charge of the pores through the PETP membrane. Thus the relative values of K_d for water (1.0), Rb^+ (1.1), Cl^- (0.6), choline (0.4), glycerol (0.3) and sucrose (0.2) are not so different from their relative diffusion coefficients, namely water, Rb^+ and Cl^- (1.0), choline (0.5), glycerol (0.45) and sucrose (0.3). As the pores become narrower, the values of K_d decrease accordingly: K_d for all molecules decreases 7–8-fold between the 50-min-etched and the 20-min-etched membrane; the decrease between the 20-min-etched membrane and the 10-min-etched membrane is more variable, due to the effect of surface charge and — in the case of choline — the effect of size (*see* Table 7 below). As mentioned above, effects of surface charge in 0.16 M salt become manifest only in the 10-min-etched membrane, as a result of which K_d for Cl^- is decreased relatively more than that for Rb^+ or choline. The selectivity of membranes etched for different times is shown in Table 6. The agreement with values of selectivity that were calculated from measurements of reversal potential (t_+) is reasonable.

We may summarize the effect of etching time on the diffusion of ions as follows. In the 10-min-etched membrane, the pores are of such a width as to make the difference between K_d for cations and anions appreciable at 0.16 M salt; the difference disappears in 1 M salt. In the 20-min-etched membrane, the pores appear to be some 10 times larger in area, according to the diffusion of water, and the difference is seen at 0.01 M (but less in 0.16 M) salt. In the 50-min-etched membrane, the pores are some 7 times larger again and the difference is seen at 0.001 M (but less in 0.01 M) salt. Since increased time of etching is likely to create at least as many — not fewer — negative charges at the pore surface by hydrolysis of ester bonds, it is likely that the differential rate of diffusion between cations and anions is not so much *abolished* as pore size increases, but rather *swamped* by the relatively larger contribution of ''bulk flow''; this interpretation is compatible with the effect of ionic strength

Table 6. Effect of etching time and methylation on ionic selectivity

Panel A Ions	Untreated			Methylated		
	Time of etching			Time of etching		
	10 min	20 min	50 min	10 min	20 min	50 min
	(sel_d)			(sel_d)		
$^{86}Rb^+$ *vs.* $^{36}Cl^-$	0.91 (6)	0.71 (5)	0.66 (2)	0.74	0.57 (2)	0.54 (2)
[^{3}H]choline *vs.* $^{36}Cl^-$	0.86 (3)	0.50 (6)	0.41 (2)	0.70 (3)	0.39 (3)	0.37 (2)

Panel B Ions	Gradient	Untreated			Methylated		
		Time of etching			Time of etching		
		10 min	20 min	50 min	10 min	20 min	50 min
		(t_+)			(t_+)		
K^+ *vs.* Cl^-	0.1/0.5 M	0.91	0.87	0.80	0.63		
	0.1/0.3 M	0.83 ± 0.04 (13)	0.77 ± 0.03 (23)	0.63 ± 0.04 (32)	0.60 ± 0.04 (6)	0.49 ± 0.08 (23)	0.52 ± 0.01 (33)
Choline *vs.* Cl^-	0.1/0.3 M	0.92 ± 0.08 (9)	0.88 ± 0.07 (15)	0.65 ± 0.05 (16)		0.66 ± 0.05 (15)	0.51 ± 0.03 (8)

All experiments were performed on pieces of PETP membrane that had been etched for the times indicated and parts of which were subsequently methylated.

Panel A: All experiments were performed in 0.16 M salt (NaCl, KCl or choline Cl) by the ''dynamic technique'' on the three pieces used for the experiments described in Table 5 (untreated) and a similar series for the methylated membranes. For $^{86}Rb^+$ *vs.* $^{36}Cl^-$, the values of sel_d were calculated from the mean values of K_d for $^{86}Rb^+$ and the mean values of K_d for $^{36}Cl^-$ (numbers in parentheses refer to the number of experiments; where these are different for $^{86}Rb^+$ and $^{36}Cl^-$, the lower number is given). For [^{3}H]choline *vs.* $^{36}Cl^-$ the values of sel_d were calculated from individual ''double label'' experiments (number in parentheses) carried out on the same piece of membrane in which K_d for [^{3}H]choline and $^{36}Cl^-$ was measured simultaneously.

Panel B: Selectivity of ion current, t_+, was measured and calculated as described in Materials and Methods. Experiments in 0.1/0.5 M KCl were performed on 1-cm^2 pieces of membrane; experiments in 0.1/0.3 M salt were performed on (app.) 1 μm^2 patches (±SD with number of patches in parentheses).

referred to above.

The effect of etching time on the diffusion of neutral solutes is shown in Table 7, which also lists the diffusion coefficients of the solutes in free solution. It would appear that the diffusion of solutes as small as urea is limited by the average pore size of the 10-min-etched membrane (''molecular sieving''), that diffusion of solutes larger than urea is limited in the 20-min-etched membrane, but that there is little limitation in the 50-min-etched membranes for solutes as large as sucrose.

The exclusion technique (Fig. 4) indicates a ''cutoff size'' corresponding to a molecular weight of PEG intermediate between 600 and app. 10,000 daltons for the 10-min-etched membrane. This indicates (Krasilnikov et al, 1992) an average pore radius of between 0.6 and 1.8 nm. Such a radius is clearly incompatible with the fact that urea does not freely penetrate the membrane (Table 7). Moreover for the 20-min-etched membrane, the value of *A* does not approach zero, but flattens out at approx. 0.55 (Fig. 4). These discrepancies are likely to arise from the fact that the pores are not cylindrical, but double funnel or elongated ''egg-timer'' shaped (*see* Fig. 5 below): the resistance in terms of ion current (or of absolute rates of diffusion) depends not only on the radius of the narrower portion in the center of the membrane, but on the relationship between that portion, the radius of the mouth of the pore, and the height of the funnel (which is half the thickness of the membrane, i.e., 5 μm or approx. 1,000 times longer than the radii at its two ends). Ion current (or rate of diffusion) will depend on the geometry of such funnels, into which molecules of between 600 and 10,000 daltons (in the case of 10-min-etched membrane, and >35,000 daltons in the case of 20 min and 50-min-etched membranes) will penetrate to different extents. Approximate values for the two radii of such funnel-shaped pores are derived below (Discussion).

Effect of Methylation

The effect of reducing surface charge in etched PETP membranes by methylating free carboxyl groups (cf. Mackinnon, Latorre & Miller, 1989) has been studied. First, there is no apparent change in pore size when this

Table 7. Effect of etching time on diffusion of nonelectrolytes

Tracer	Time of etching			Molecular weight	Diffusion in free solution	Approx. size‡
	10 min	20 min	50 min			
	(K_d)				(D)	(R)
^3H_2O	100*	100*	100*	18	100†	0.14
[^{14}C]urea	7	48 (4)		60	49	0.22
[^{14}C]glycerol	6	27 (3)	30	92	39	0.29
Glc				180	23	0.4
[^{14}C]MeGlc		14 (9)		194		
[^{14}C]sucrose	4	10 (3)	20	342	18	0.5

All experiments were performed on pieces of PETP membrane that had been etched for the times indicated. Experiments were performed in 0.01 M, 0.1 M or 0.16 M salt, by the ''static'' or ''dynamic'' technique, and averaged (number in parentheses). Experiments by the ''dynamic'' technique were with the same three pieces used for the experiments described in Tables 5 and 6.

* The K_d values for ^3H_2O were as shown in Table 5, *viz.* 2.9×10^{-4} (5), 2.6×10^{-3} (7) and 1.9×10^{-2} (4) in the 10-min-, 20-min- and 50-min-etched membrane respectively.

† Based on a diffusion coefficient (D) for H_2O of 2.1×10^{-5} cm$^2 \cdot$ sec^{-1} taken from p. 280 of Hille (1992); values for urea and glycerol from p. 338 of the same source; values for glucose and sucrose from Weast (1986).

‡ Radius (r) in nm assuming a spherical molecule of the dimensions given by Finkelstein (1984) or Stein (1986), that are in broad agreement with values quoted by Bean (1972).

is measured by the PEG exclusion technique (Fig. 4): the curves for methylated and unmethylated 10-min-etched membrane — in which any differences due to methylation are likely to be greatest (*see* Table 8 below) — are identical. This result is in keeping with the fact that methylation has no effect on the diffusion of water through the 20-min- or 50-min-etched membranes; diffusion of water through the 10-min-etched membrane, however, is markedly reduced by methylation (Table 8). If, as suggested by PEG exclusion, pore size is unaffected by methylation, the latter observation may be partly a consequence of a relative increase in hydrophobicity at the surface of a methylated pore: the effect is swamped in relatively wide pores (20-min and 50-min-etched) but appreciable in a narrow pore (10-min-etched). So far as the diffusion of ions is concerned, the effect of methylation appears to be twofold: first, the difference between diffusion of cations and anions — i.e., selectivity — is decreased (but not abolished, presumably because methylation of carboxyl groups is not 100% complete) (Table 6). Second, there is an actual decrease in the diffusion of Cl^- (in the 10-min-etched membrane) (not an increase, as might be expected); the diffusion of Rb^+ is decreased even more (Table 8). This ''extra'' decrease in ionic diffusion is presumably related to the decreased water diffusion, namely a consequence of the hydrophobic effect in such narrow pores that was referred to above.

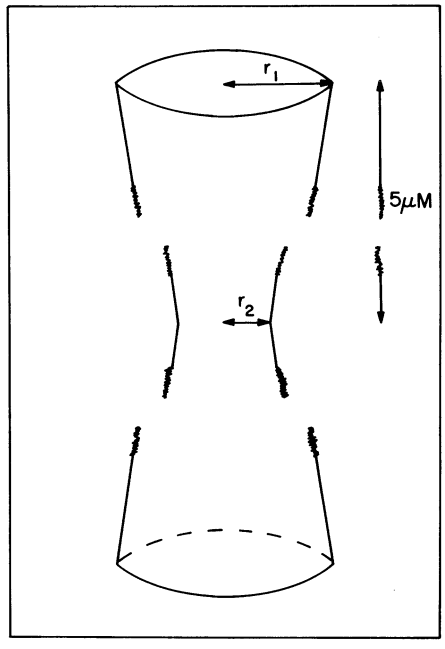

CAP 170

Fig. 5. Model for an average pore in a track-etched PETP membrane. r_1 is the radius of the pore at the membrane surface (mouth) and r_2 is the radius in the center of the membrane; only a small portion of the pore in the center of the membrane and at each mouth is represented. For membranes etched for 10 min $r_1 \approx 3$ nm, $r_2 \approx 0.3$ nm; for membranes etched for 20 min $r_1 \approx 9$ nm, $r_2 \approx 1$ nm; for membranes etched for 50 min $r_1 \approx 23$ nm, $r_2 \approx 3$ nm.

Discussion

Track-etched PETP membranes containing app. 1 pore/cm^2 are proving to be a useful model for studying single

Table 8. Effect of methylation on diffusion of ions, water and MeGlc

Tracer	Time of etching		
	10 min	20 min	50 min
	(K_d as % of unmethylated)		
$^{86}Rb^+$	4 (6)	89 (2)	80
[^{3}H]choline	32 (3)	94 (6)	86 (2)
$^{36}Cl^-$	14 (4)	117 (7)	101 (5)
^3H_2O	13 (2)	53	73 (2)
[^{14}C]MeGlc		126 (2)	

All experiments were performed in 0.16 M salt by the ''dynamic'' technique on the same pieces used for experiments described in Table 6, panel *A*. The K_d values for the different tracers used with untreated membranes are taken from Table 2 and Table 4. Number of experiments in parentheses.

ion channels and pores through biological membranes: they display fluctuations of ion current between discrete conductance states, selectivity of ion current between cations and anions, and sensitivity to pH and divalent cations (Lev et al., 1993). Track-etched PETP membranes containing app. 10^9 pores/cm^2 show the same properties in respect of selectivity and sensitivity to pH and divalent cations (Pasternak et al., 1993) and, when individual pores are studied with a patch-pipette, show fluctuations of ion current as well (Pasternak et al., 1995*a*,*b*). The fact that the pores have a nominal length some 10^3-fold greater than those through biological channels seems not to affect these properties; what matters is that their cross-sectioned area — corresponding to a radius of 1-10 nm — is of the same dimension as that of certain endogenous channels (Loewenstein, 1981; Blachly-Dyson et al., 1990) and many toxin-induced pores (Bhakdi & Tranum-Jensen, 1987). Because the pores in PETP membranes are fixed and stable within the membrane, the same pores can be studied by a variety of techniques. Here we report on the diffusion of ions, water and nonelectrolyte through membranes containing app. 10^9 pores/cm^2 that have been etched for 10, 20 and 50 min to produce pores of increasing size. Our results are in general agreement with an earlier study (Pasternak et al., 1993) in which a track-etched PETP membrane containing pores that were of greater heterogeneity than those in the present samples, was studied. Because the rate of diffusion of ions and other molecules was dominated by a small number of relatively large pores, lipid was added to ''narrow'' these. One effect of the lipid was to increase the diffusion of water relative to that of ions. Other discrepancies between the behavior of lipid-treated and lipid-free PETP membranes are under study. The overall results of our measurements are quite compatible with models based on many previous studies of diffusion and flow through narrow pores (e.g., Bean 1972; Anderson & Quinn, 1974), especially in regard to the concept of ''surface conductance'' that is based on the existence of an electrical double layer at a charged surface (e.g., Davies & Rideal 1961; Lakshminarayanaiah, 1969).

There is much information on the rate of water flow — both diffusional and osmotic — through lipid bilayers, through biological membranes and through pores induced by antibiotics such as gramicidin, nystatin or amphotericin (Finkelstein, 1984). Because of the high rate of water movement through lipids — diffusional water permeability coefficients (P_d) as high as 10^{-2} cm/sec have been recorded (Huang & Thompson 1966) — this dominates flow through biological membranes (of around 2×10^{-3} to 2×10^{-2} cm/sec); that is, flow through ion and other channels contributes relatively little to the observed flow of water across the plasma membrane of most cells (Finkelstein, 1984); erythrocytes appear to be an exception to this generalization (Fettiplace & Haydon, 1980) and specific water channels (''aquaporins'') have indeed been identified in such cells (Chrispeels & Agre, 1994). So far as flow of water through antibiotic-induced pores is concerned, values of p_d (the diffusional permeability coefficient per pore) of around 10^{-14} cm^3/sec have been recorded (Finkelstein, 1984). These values for P_d and p_d may be compared with the present data, which gives values for water diffusion through the 20-min-etched membrane (based on K_d of 2×10^{-3}/min/cm^2 of $P_d = 1.4 \times 10^{-5}$ cm/sec and $p_d = 1.4 \times 10^{-14}$ cm^3/sec. Those values are not corrected for the unstirred layer on either side of the membrane (Holz & Finkelstein, 1970): we assume their contribution to P_d or p_d to be less than 10% for water, ions or nonelectrolytes because they do not penetrate unetched membranes and the porosity of the longest-etched membrane is less than 2% (1.6% for the 50-min-etched membrane). What is surprising is that the values of p_d for water diffusion through antibiotic-induced pores and through PETP membranes are so close. For although the pores in etched PETP membranes have apparent radii similar to pores induced across biological membranes (*see below*), their length (10 μm) is ~1,000 times greater than that across a biological membrane (app. 10 nm). Yet the radii of pores through etched PETP membranes that are obtained when absolute rates of diffusion are calculated (assuming a cylindrical shape) (Fig. 6 *below*) are remarkably close to those based on independent measurements (Fig. 5; *see below*) which suggests that our measurements of p_d are correct. This again emphasizes the potential usefulness of track-etched PETP membranes as models for endogenous pores through biological membranes.

Pores through etched PETP membranes are not, in fact, true cylinders, but have a taper towards the middle, giving them an ''elongated egg-timer'' shape. The reason is that the etchant (hot alkali), which acts from both sides of the membrane, has a small lateral component as well as a large vertical one along the tracked, i.e., damaged, area of the membrane (e.g., Spohr, 1990). Hence it

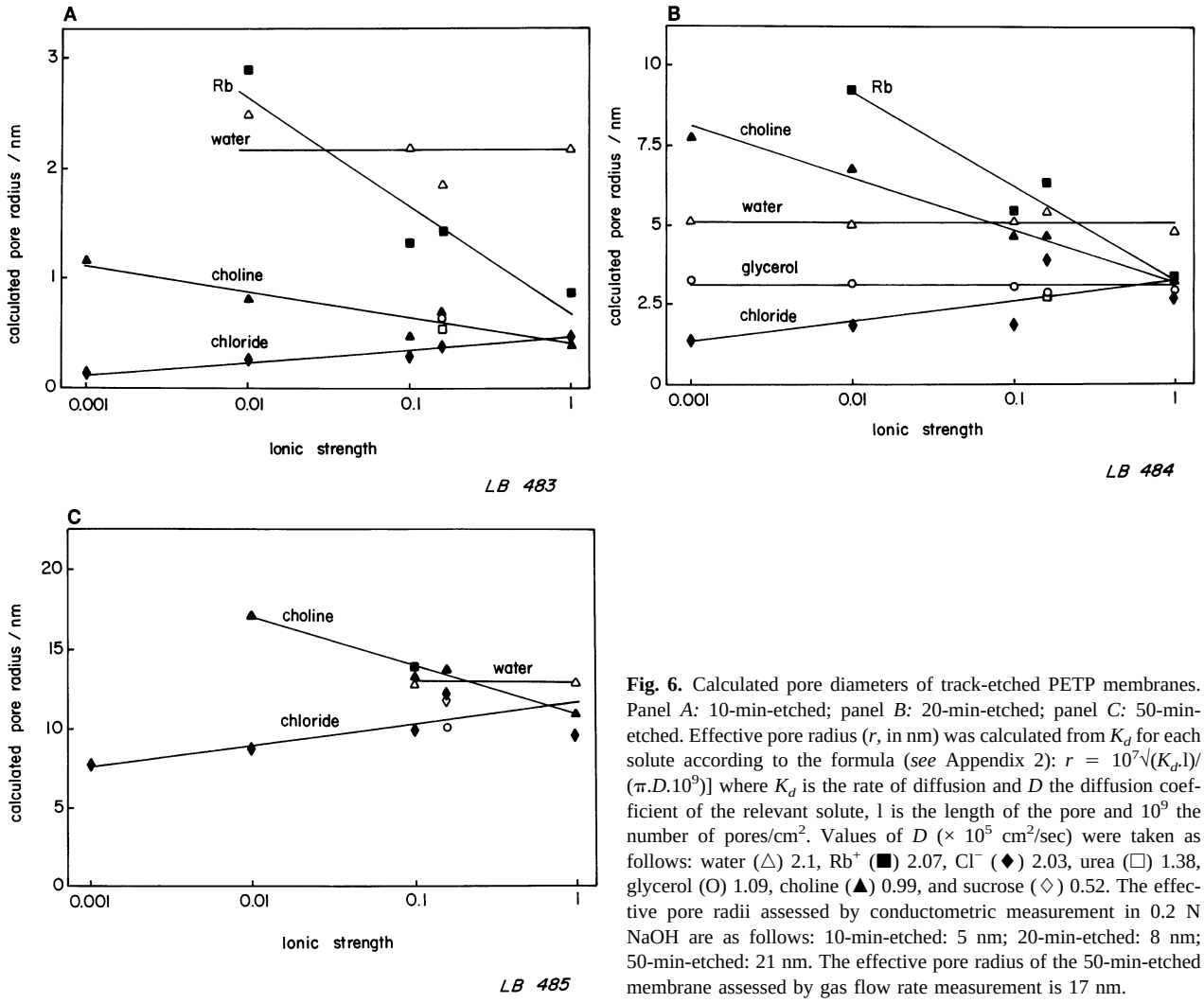

Fig. 6. Calculated pore diameters of track-etched PETP membranes. Panel *A:* 10-min-etched; panel *B:* 20-min-etched; panel *C:* 50-min-etched. Effective pore radius (r, in nm) was calculated from K_d for each solute according to the formula (*see* Appendix 2): $r = 10^7\sqrt{(K_d.l)/(\pi.D.10^9)}$] where K_d is the rate of diffusion and D the diffusion coefficient of the relevant solute, l is the length of the pore and 10^9 the number of pores/cm^2. Values of D ($\times 10^5$ cm^2/sec) were taken as follows: water (△) 2.1, Rb^+ (■) 2.07, Cl^- (♦) 2.03, urea (□) 1.38, glycerol (O) 1.09, choline (▲) 0.99, and sucrose (◇) 0.52. The effective pore radii assessed by conductometric measurement in 0.2 N NaOH are as follows: 10-min-etched: 5 nm; 20-min-etched: 8 nm; 50-min-etched: 21 nm. The effective pore radius of the 50-min-etched membrane assessed by gas flow rate measurement is 17 nm.

produces pores that have a radius at their center that is — for the lightly etched membranes used in this study — as little as appr. 10% of that at the two ends. Such a structure reconciles the apparent discrepancy between relative diffusion (Table 7) and PEG exclusion (Fig. 4): small molecules like sucrose may not penetrate a pore because they cannot pass the narrowest portion in the middle, yet much larger molecules like PEG 10,000 are able to enter the mouth, and hence affect overall ion conductance through the pore. This results in broader PEG exclusion curves due to hindered penetration (Deen, 1987) than those obtained, for example, with *S. aureus* α-toxin (Krasilnikov et al., 1988; Korchev et al., 1995) for which the pore is some 1,000-fold shorter. As membranes are etched for progressively longer times their taper becomes less significant, and their appearance becomes progressively more cylindrical. Electron micrographs of pores with radii longer than 0.1 μm show just that (e.g., p2 of Spohr, 1990). As yet it has not been possible to image the types of narrow pore investigated in this study.

The shape of such pores, that best fits the experimental data, is shown in Fig. 5. The dimensions are based on the following assumptions: (i) the vertical (''track'') etching rate is app. 2,500 nm/min, with a ''breakthrough'' time of 2—5 min, and the lateral etching rate is app 0.5 nm/min (Apel, 1995); (ii) the relative rate of water diffusion increased 9-fold between a 10-min- and a 20-min-etched membrane and 7-fold between a 20-min- and a 50-min-etched membrane (Table 5), indicative of 3-fold and 2.6-fold increases in radius, resp.; (iii) urea barely penetrates the 10-min-etched membrane (Table 7), but solutes as large as 10,000 dalton PEG (app. radius 1.8 nm) affect its conductivity (Fig. 4); (iv) sucrose penetrates the 20-min-etched membrane only slightly (Table 7), but solutes as large as 35,000 dalton PEG (app. radius 2.8 nm) affect its conductivity (Fig. 4); (v) solutes as large as 35,000 dalton penetrate the 50-min-etched membrane (Fig. 4); (vi) observed values of P_d fit a cylinder of radius 2 nm (water diffusion) or 0.5 nm (solute diffusion) in the case of the 10-min-etched

membrane, 5 nm (water diffusion) or 3 nm (solute diffusion; also ion diffusion at high ionic strength) in the case of the 20-min-etched membrane and 13 nm (water diffusion) or 10 nm (solute diffusion; also ion diffusion at high ionic strength) in the case of the 50-min-etched membrane (Fig. 6); as noted by Bean (1972), a cylindrical pore model accounts reasonably well — to within a factor of 2 — for the observed diffusion of solutes through various membranes. From such radii for a cylinder, app. values for r_1 and r_2 that are respectively greater and less than the cylindrical radius, may be derived (Fig. 5).

The lining of the pore (as well as the two surfaces of the membrane) is not smooth, but contains protrusions that may extend as much as 100 nm away from the rest of the surface; these protrusions may be penetrated by water but not by ions or other solutes (Fig. 6 and data of Y.E. Korchev in London and P.Y. Apel in Dubna). In the cases where such protrusions affect diffusion rates significantly (i.e., the central portions of the shortest-etched membranes) the values of r_2 will correspond to the distance from the center to the edge of the protrusion, rather than the distance to the rest of surface. The fact that such protrusions may expand in aqueous solutions may explain the erratic behavior of the 20-min-etched membrane (*see* Results: comparison between 'static; and 'dynamic' technique); the 10-min-etched membrane (and a 5-min-etched membrane) display similar behavior: that is, diffusion of ions or water, as well as ion current, often decreased markedly from an initially high value to a lower value that is difficult to reverse in the shortest-etched membranes.

Relatively few studies on solute flow through endogenous channels or through antibiotic- or toxin-induced pores have been reported. One interesting example is afforded by the cytolytic toxin from the sea anemone *Stoichactis helianthus:* this forms relatively stable pores across planar lipid bilayers and the diffusion of urea, glycerol, glucose and sucrose through them has been measured: P_d values of 3.2, 2.6, 0.85 and 0.21 × 10^{-6} cm/sec respectively were recorded (Varanda & Finkelstein, 1980). These may be compared with P_d values of 3.4, 1.9, 1.0 and 0.7 × 10^{-6} cm/sec for urea, glycerol, MeGlc and sucrose respectively for the 20-min-etched membrane (Table 7). The size of the toxin pore (estimated to be > 0.5 nm radius on the basis that sucrose does penetrate) is similar to that of the narrowest part of the 20-min etched PETP membrane, estimated to be app. 1 nm (Fig. 5). Since PETP pores are some 1,000-fold longer than toxin pores, the agreement probably means that there were some 1,000-fold more toxin pores per unit area of membrane than in the case of PETP. As mentioned above, calculation of the absolute rates of diffusion of nonelectrolytes based on a cylinder gives a radius — *viz.* 3 nm for the 20-min-etched membrane — that is quite compatible with the radii of an equivalent (in volume) ''elongated egg-timer,'' namely 1 nm at the center and 9 nm at each end (Fig. 5).

The diffusion of ions — unlike that of water or nonelectrolytes — is strongly influenced by ionic strength, by pH and by the presence of divalent cations (Tables 2, 3, 7 and 8 and Fig. 2). At sufficiently low ionic strength, the diffusion of Rb^+ is some 20-fold faster than that of Cl^-; the ionic strength necessary to observe this difference depends on the size of pore: in the 10-min-etched membranes, a 3-fold faster rate of diffusion (for choline *vs.* Cl) is seen even at 1M (K_d 8.2 × 10^{-6} *vs.* 2.6 × 10^{-6}); in the 20-min-etched membrane, the ionic strength needs to be < 0.1 M to observe a difference (Fig. 2); in the 50-min-etched membrane it needs to be < 0.001 M K_d (1.4 × 10^{-2} *vs.* 4.4 × 10^{-3} at 0.001 M). This effect is explicable in terms of the screening efficacy of the cations present in solution (whether K^+, Rb^+, Na^+ or choline) on the fixed negative charges along the walls of the pores: at 1 M salt the Debye length of a univalent charge is ~ 0.3 nm. Debye length increases as the ionic strength is reduced (at 0.1 M it is ~ 1 nm; at 0.01 M it is ~ 3 nm and at 0.001 M it is ~ 10 nm); since differential flow or ''surface flow'' may be expected to occur only within the Debye length, the contribution of ''surface flow'' to ''bulk flow'' will depend on the overall size of the pore. Such a model to explain altered selectivity (of ion current) with altered ionic strength has been presented (Zambrowicz & Colombini, 1993) in relation to the voltage-dependent anion channel (VDAC) of mitochondria, that has a pore radius of about 1.5 nm (Blachly-Dyson et al., 1990). In contrast, there are channels in which selectivity of ion current is achieved for reasons *other* than surface charge (e.g., Kienker & Lear, 1995).

By being able to measure rates of diffusion of cations and anions independently, we are able to compare these with the diffusion of water (and nonelectrolytes) to answer the following question: can the rate of ''surface flow'' (measured as rate of diffusion) of cations be faster than that of ''bulk flow'' (i.e., diffusivity)? It would appear to be so: a quick glance at Table 1 indicates that (for the 20-min-etched membrane in 0.01 M KCl), diffusion of Rb^+ is some 4 times faster than that of water, yet its diffusivity in free solution — like that of K^+ or Cl^- is the same as that of water (app. 2 × 10^{-5} cm^2/sec). As expected, in the 50-min-etched membrane in 0.16 M KCl, the rates of diffusion of Rb^+, Cl^- and water are similar, with that for choline and MeGlc being less, consistent with their lower diffusivity in free solution.

In summary, tracked PETP membranes that have been etched for different times to produce pores of increasing size have proved useful for defining the conditions under which ''surface flow'' is manifest. These are: (i) a charged surface and (ii) an ionic strength such that the distance from the surface at which the charge is felt

is commensurate with the radius of the pore. ''Surface flow'' applies to ions, not to water or nonelectrolytes: a negative surface causes cations to diffuse faster — and anions to diffuse slower — than they would in free solution because the former are concentrated, and the latter excluded, by the surface. Such pores across membranes act catalytically to accelerate the diffusion of ions across the membrane; in the presence of an electric potential across the membrane, current — carried predominantly by the faster-diffusing ion — will flow faster than it would in free solution; this is what is referred to as ''surface conductance.''

We are grateful to Drs. Donald Edmonds and Yuri Korchev for stimulating discussion, to Barbara Bashford and Stefanina Pelc for preparing the paper and to the Biotechnology and Biological Sciences Research Council (BBSRC), Cell Surface Research Fund, Molecular and Cell Biology Network of UNESCO, the National Institutes of Health (Fogarty MIRT Program) and The Wellcome Trust for financial support.

References

Andersen, J.L., Quinn, J.A. 1974. Restricted transport in small pores. *Biophys. J.* **14:**130–150

Apel, P.Y. 1995. Heavy particle tracks in polymers and polymeric track membranes. *Radiation measurements* **25:**667–674

Apel, P.Y., Kuznetsov, V.I., Zhitariuk, N.I., Orelovich, O.L. 1985. Nuclear ultrafilters. *Kolloidnyi zhurnal* (USSR) (Engl. trans *Colloid J.*) **47:**1–5

Bashford, C.L., Menestrina, G., Henkart, P.A., Pasternak, C.A. 1988. Cell damage by cytolysin. Spontaneous recovery and reversible inhibition by divalent cations. *J. Immunol.* **141:**3965–3974

Bean, C.P. 1972. The physics of porous membranes. *In:* Membranes. G. Eisenman, editor. pp 1–54. Marcel Dekker, New York

Bhakdi, S., Tranum-Jensen, J. 1987. Damage to mammalian cells by proteins that form transmembrane pores. *Rev. Physiol. Biochem. Pharmacol.* **107:**147–223

Blachly-Dyson, E., Peng, S., Colombini, M., Forte, M. 1990. Selectivity changes in site-directed mutants of the VDAC ion channel: structural implications. *Science* **247:**1233–1236

Chrispeels, M.J., Agre, P. 1994. Aquaporins: water channel proteins of plant and animal cells. *Trends Biochem. Sci. (TIBS)* **19:**421–425

Colowick, S.P., Womack, F.C. 1969. Binding of diffusible molecules by macromolecules: rapid measurement by rate of dialysis. *J. Biol. Chem.* **244:**774–777

Davies, J.T., Rideal, E.K. 1961. Interfacial Phenomena. pp. 108–153. Academic Press, New York

Deen, W.M. 1987. Hindered transport of large molecules in liquid-filled pores. *Am. Inst. Chem. Engin. J.* **33:**1409–1425

Donovan, J.J., Simon, M.I., Draper, R.K., Montal, M. 1981. Diphtheria toxin forms transmembrane channels in planar lipid bilayers. *Proc. Natl. Acad. Sci. USA* **78:**172–176

Feldman, K. 1978. New devices for flow dialysis and ultrafiltration for the study of protein ligand interactions. *Anal Biochem.* **88:**225–235

Fettiplace, R., Haydon, D.A. 1980. Water permeability of lipid membranes. *Physiol. Rev.* **60:**510–550

Finkelstein, A. 1984. Water movement through membrane channels. *Current Topics Membr. Transport* **21:**295–308

Gambale, F., Montal, M. 1988. Characterization of the channel properties of tetanus toxin in planar lipid bilayers. *Biophys. J.* **53:**771–783

Hille, B. 1992. Ionic channels of excitable membranes. (2nd ed). Sinauer Associates, Sunderland, MA

Holz, R., Finkelstein, A. 1970. The water and nonelectrolyte permeability induced in thin lipid membranes by the polyene antibiotics nystatin and amphotericin B. *J. Gen. Physiol.* **56:**125–145

Huang, C., Thompson, T.E. 1966. Properties of lipid bilayer membranes separating two aqueous phases: Water permeability. *J. Mol. Biol.* **15:**539–554

Kagan, B.L., Finkelstein, A., Colombini, M. 1981. Diphtheria toxin fragment forms large pores in phospholipid bilayer membranes. *Proc. Natl. Acad Sci. USA* **78:**4950–4954

Kasianowicz, J.J., Bezrukov, S.M. 1995. Protonation dynamics of the α-toxin ion channel from spectral analysis of pH-dependent current fluctuations. *Biophys. J.* **69:**94–105

Kienker, P.K., Lear, J.D. 1995. Charge selectivity of the designed uncharged peptide ion channel Ac-$(LSSLLSL)_3$-$CONH_2$. *Biophys. J.* **68:**1347–1358

Korchev, Y.E., Bashford, C.L., Alder, G.M., Kasianowicz, J.J., Pasternak, C.A. 1995. Low conductance states of a single ion channel are not 'closed'. *J Membrane Biol.* **147:**233–239

Krasilnikov, O.V., Sabirov, R.Z., Ternovsky, V.I., Merzliak, P.G., Muratkhodjaev, J.N. 1992. A simple method for the determination of the pore radius of ion channels in planar lipid bilayer membranes. *FEMS Microbiol. Immunol.* **5:**93–100

Krasilnikov, O.V., Sabirov, R.Z., Ternovsky, V.I., Merzliak, P.G., Tashmukhamedov, B.A. 1988. The structure of *Staphylococcus aureus* alpha-toxin-induced ionic channels. *Gen. Physiol. Biophys.* **7:**467–473

Kuga, S. 1981. Pore-size distribution analysis of gel substances by size exclusion chromatography. *J Chromat.* **206:**449–461

Lakshminarayanaiah, N. 1969. Transport Phenomena in Membranes. Academic Press, New York

Lev, A.A., Korchev, Y.E., Rostovtseva, T.K., Bashford, C.L., Edmonds, D.T., Pasternak, C.A. 1993. Rapid switching of ion current in narrow pores: implications for biological ion channels. *Proc. R. Soc. B* **252:**187–192

Loewenstein, W.R. 1981. Junctional intercellular communication: the cell-to-cell membrane channel. *Physiol. Rev.* **61:**829–913

MacKinnon, R., Latorre, R., Miller, C. 1989. Role of surface electrostatics in the operation of a high-conductance Ca^{2+}-activated K^+ channel. *Biochemistry* **28:**8092–8099

Meares, P., Page, K.R. 1974. Oscillatory fluxes in highly porous membranes. *Proc. R. Soc. Lond. A.* **339:**513–532

Menestrina, G. 1986. Ionic channels formed by *Staphylococcus aureus* alpha-toxin: Voltage-dependent inhibition by divalent and trivalent cations. *J. Membrane Biol.* **90:**177–190

Menestrina, G., Pasquali, F. 1985. Reconstitution of the complement channel into lipid vesicles and planar bilayers starting from the fluid phase complex. *Biosci. Rep.* **5:**129–136

Michaels, D.W. 1979. Membrane damage by a toxin from the sea anemone *Stoichactis helianthus. Biochim. Biophys. Acta* **555:**67–78

Pasternak, C.A., Alder, G.M., Apel, P.Y., Bashford, C.L., Edmonds, D.T., Korchev, Y.E., Lev, A.A., Lowe, G., Milovanovich, M., Pitt, C.W., Rostovtseva, T.K., Zhitariuk, N.I. 1995*a*. Nuclear track-etched filters as model pores for biological membranes. *Radiation Measurements* **25:**675–683

Pasternak, C.A., Alder, G.M., Apel, P.Y., Bashford, C.L., Korchev, Y.E., Lev, A.A., Rostovtseva, T.K., Zhitariuk, N.I. 1995*b*. Model pores for biological membranes: the properties of track-etched membranes. *Nuclear Instruments and Methods in Physics Research B.* Elsevier (*in press*)

Pasternak, C.A., Bashford, C.L., Korchev, Y.E., Rostovtseva, T.K.,

Lev, A.A. 1993. Modulation of surface flow by divalent cations and protons. *Colloids + Surfaces. A: Physicochemical and Engineering Aspects.* **77:**119–124

Powell, G.M. 1980. Polyethyleneglycol. *In:* Handbook of Water-Soluble Gums and Resins. R.L. Davidson, editor. pp. 18-1 – 18-31. McGraw Hill, New York

Raymond, L. Slatin, S.L., Finkelstein, A. 1985. Channels formed by colicin E1 in planar lipid bilayers are large and exhibit pH-dependent ion selectivity. *J. Membrane Biol.* **84:**173–181

Root, M.J., MacKinnon, R. 1994. Two identical noninteracting sites in an ion channel revealed by proton transfer. *Science* **265:**1852–1856

Spohr, R. 1990. *Ion Tracks and Microtechnology*. F. Vieweg and Son, Braunschweig, Germany

Stein, W.D. 1986. Transport and diffusion across cell membranes. pp. 128, 149. Academic Press, Orlando, FL

Tosteson, M.T., Tosteson, D.C. 1981. The sting. Melittin forms channels in lipid bilayers. *Biophys. J.* **36:**109–116

Unwin, N. 1995. Acetylcholine receptor channel imaged in the open state. *Nature* **373:**37–43

Varanda, W., Finkelstein, A. 1980. Ion and non-electrolyte permeability properties of channels formed in planar lipid bilayer membranes by the cytolytic toxin from the sea anemone, *Stoichactis helianthus. J. Membrane Biol.* **55:**203–211

Weast, R.C. 1986. CRC Handbook of Chemistry and Physics. 67th edition. p. F-45. CRC Press, Boca Raton, FL

Young, J.D.E., Leong, G.L., Liu, C-C., Damiano, A., Cohn, Z.A. 1986. Extracellular release of lymphocyte cytolytic pore-forming protein (perforin) after ionophore stimulation. *Proc. Natl. Acad. Sci. USA* **83:**5668–5672

Zambrowicz, E.B., Colombini, M. 1993. Zero-current potentials in a large membrane channel: a simple theory accounts for complex behaviour. *Biophys. J.* **65:**1093–1100

Appendix 1

Menestrina (1986) gives a general expression for reversal potential from which:

$$\psi = V_{rev} = (kT/e)\Sigma_i [(t_i/z_i)\ln(f_i c_i/f'_i c'_i)] = \Sigma_i[(t_i/z_i)\ \psi_i]$$

where t_i, z_i and ψ_i are the transference number, valence and Nernst potential for the ith ion, unprimed letters stand for one side (*cis*) of the membrane and primed letters for the other side (*trans*).

$$\begin{aligned}
\ln \mathrm{KCl}\ \psi &= t_- \psi_{\mathrm{Cl}} + t+\psi_{\mathrm{K}} \\
\text{As } 1 &= t_+ + t_- \\
\text{Then } \psi &= (1 - t_+)\psi_{\mathrm{Cl}} + t_+\psi_K \\
\text{and } t_+ &= (\psi - \psi_{\mathrm{Cl}})/(\psi_K - \psi_{\mathrm{Cl}}) \\
\text{in KCl } \psi_{\mathrm{Cl}} &= -\psi_{\mathrm{K}} \\
\text{therefore } t_+ &= (\psi + \psi_K)/2\psi_K \\
t_+ &= 0.5(1 + \psi/\psi_K) \\
t_+ &= 0.5\{1 + \psi/([RT/F]ln([K^+]trans/[K^+]cis))\}
\end{aligned}$$

Appendix 2

Unidirectional flux (ϕ_p) through a cylindrical pore (Bean, 1972; Hille, 1992) is given by:

$$\phi_p = \pi r^2 D\Delta c/(l + \pi r/2) \quad \text{(A1)}$$

where r is the radius and l the length of the cylinder, D is the diffusion coefficient of the solute and Δc is the difference in concentration of the solute at either end of the cylinder; when $l \gg r$ equation (1) simplifies to:

$$\phi_p = \pi r^2 D\Delta c/\mathrm{l} \quad \text{(A2)}$$

In 'dynamic' experiments, tracer concentration on the 'cold' side is kept zero thus Δc represents the concentration of the tracer-labeled solute on the 'hot' side.

Solute flux (ϕ_{sol}) across the membrane is given by:

$$\phi_{sol} = K_d.c.v \quad \text{(A3)}$$

where c is the concentration of solute in and v the volume of the upper chamber. Flux per pore is the flux per membrane divided by the number of pores. In our 'dynamic' experiments:

$$\phi_p = K_d.c.v/10^9 \quad \text{(A4)}$$

substituting in Eq. 2 and rearranging yields:

$$r = \sqrt{(K_d.\mathrm{l}/\pi.\mathrm{D}.10^9)} \quad \text{(A5)}$$